Interface barriers for flux motion in high-temperature superconducting superlattices

J. E. Villegas,[1] Z. Sefrioui,[2] M. Varela,[2,*] E. M. Gonzalez,[1] J. Santamaria,[2] and J. L. Vicent[1]
[1]*Departamento de Física de Materiales, Facultad CC. Fisicas, Universidad Complutense, 28040 Madrid, Spain*
[2]*GFMC, Departamento de Física Aplicada III, Facultad CC. Fisicas, Universidad Complutense, 28040 Madrid, Spain*
(Received 16 September 2003; revised manuscript received 14 January 2004; published 14 April 2004)

We study angular dependent magnetoresistance in the vortex-liquid phase of epitaxial $YBa_2Cu_3O_7$ thin films and $YBa_2Cu_3O_7/PrBa_2Cu_3O_7$ superlattices. Superlattices were grown with different $PrBa_2Cu_3O_7$ thickness in order to tune coupling between $YBa_2Cu_3O_7$ layers. While dissipation of single film and coupled superlattices is scaled with the anisotropic three-dimensional model in the whole angular range, decoupling through $PrBa_2Cu_3O_7$ spacer breaks down the scaling and yields strong reduction of the dissipation when the magnetic fields are applied up to $\pm 20°$ around the interface direction. Bean-Livingston barriers at the interface are the mechanism which governs this behavior.

DOI: 10.1103/PhysRevB.69.134505 PACS number(s): 74.72.Bk, 74.78.Bz, 74.78.Fk, 74.25.Fy

Vortex matter in high-temperature oxide superconductors (HTCS) has been extensively investigated during the last years. The mixed state properties of HTCS are governed by the interplay between the elastic properties of the vortex lattice, thermal fluctuations, and the presence of different kinds of disorder, yielding a complicated phase diagram which shows a rich variety of phenomena.[1,2] The intrinsically anisotropic structure of these oxide superconductors induces anisotropic magnetotransport properties. At magnetic fields H applied parallel to Cu-O planes the dissipation is reduced with respect to the situation where magnetic fields are perpendicular to them, due to the so-called intrinsic pinning.[3] Moreover, it has been recently shown that this anisotropic structure stabilizes a vortex smectic phase when the vortex lattice matches the periodic layered structure.[4] In this context, superconducting/insulator $YBa_2Cu_3O_7/PrBa_2Cu_3O_7$ (YBCO/PBCO) superlattices are interesting structures to artificially modify the anisotropic behavior of this HTSC.[5] This artificial manipulation yields a number of phenomena related to low dimensionality and vanishing coupling between YBCO layers,[6] vortex phase coherence,[7] dissipation anisotropy,[8] etc.

In this paper, we show that vortex pinning is enhanced in fully decoupled YBCO layers, when magnetic field is applied parallel to YBCO/PBCO interfaces. We investigate the physical origin of this behavior by studying the angular dependent dissipation in the liquid state of *c*-axis oriented YBCO/PBCO superlattices. We discuss on the interplay between intrinsic and interface pinning, and we point to surfacelike[9] barriers at the YBCO/PBCO interface as a probable origin for the observed behavior.

Epitaxial *c*-axis oriented YBCO/PBCO superlattices and YBCO single film were grown on (100) $SrTiO_3$ substrates using a high-pressure sputtering system, with stoichiometric PBCO and YBCO targets. Chamber pressure was 3.4 mbar of pure oxygen during deposition, and substrate temperature was held at 900 °C. Deposition rate was as low as $0.013\ \mathrm{nm\,s^{-1}}$, which accurately allows controlling layers thickness. The structural characterization was made by both low- and high-angle x-Ray-diffraction technique and transmission Electron microscopy. Both techniques show that superlattices have high structural quality, showing epitaxial growth without significant roughness or interdiffusion. Further details on samples fabrication and structural characterization are published elsewhere.[10,11]

Bridges (20 μm wide) were patterned by wet etching technique and the standard four probes setup was used for magnetotransport measurements. Measurements were carried out in a commercial liquid He cryostat with a superconducting 9 T solenoid. The variable temperature insert allowed controlling temperature in the range 1.5–300 K. A computer controlled rotatable sample holder was used, such that the direction of the applied magnetic field with respect to the sample could be continuously changed.

The studied samples presented sharp superconducting transitions, with critical temperatures of $T_c = 80$, 86, 88, and 90 K for samples $[YBCO_{[5\ u.c.]}/PBCO_{[5u.c.]}]_{17}$ (u.c. = unit cells), $[YBCO_{[8u.c.]}/PBCO_{[5u.c.]}]_{13}$, $[YBCO_{[17\ u.c.]}/PBCO_{[2u.c.]}]_9$, and $YBCO_{50\ nm}$ single film respectively. The total thickness of superlattices is always around 200 nm. It is important to remark that YBCO layers are fully decoupled by the five unit cells thick PBCO spacer[12–14] in the $YBCO_{[5\ u.c.]}/PBCO_{[5\ u.c.]}$ and $YBCO_{[8\ u.c.]}/PBCO_{[5\ u.c.]}$ superlattices, while they are coupled through the two unit cells thick spacer in $YBCO_{[17\ u.c.]}/PBCO_{[2\ u.c.]}$. Accordingly, in the following we will refer to superlattices with 5 PBCO u.c. spacer as the decoupled superlattices and to that with 2 PBCO u.c. as the coupled one.

In Fig. 1 is shown the angular dependence of resistance $R(\theta,H)$ at an injected current density $j = 50\ \mathrm{A\,cm^{-2}}$ in applied magnetic fields between 1 and 9 T for the four samples. $\theta = 0$ corresponds to field parallel to substrate (i.e., parallel to Cu-O planes and YBCO/PBCO interfaces). Constant Lorentz force geometry was kept by injecting electrical current in the ab plane, parallel to the rotation axis. The temperature $T = 0.99T_c$ was chosen high enough to ensure that measurements were performed above the irreversibility line for the three samples, for all fields and angles. With this purpose, isothermal *I-V* characteristics were previously measured, and the temperature for angular measurements was selected with the criterion of linear (Ohmic) *I-V* characteristic at 1 T in field parallel to Cu-O planes ($\theta = 0$) at current level range $25\ \mathrm{A\,cm^{-2}} < j < 2.5\ \mathrm{kA\,cm^{-2}}$. In Fig. 1, substantially different behavior of the four samples is observed when field is

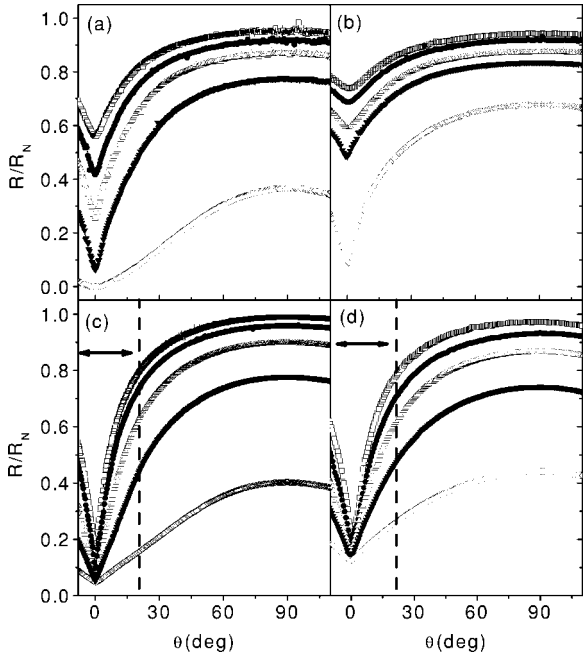

FIG. 1. Normalized resistance as a function angle of samples $YBCO_{50\ nm}$ (a) $YBCO_{[17\ u.c.]}/PBCO_{[2\ u.c.]}$ (b), $YBCO_{[8\ u.c.]}/PBCO_{[5\ u.c.]}$ (c), and $YBCO_{[5\ u.c.]}/PBCO_{[5\ u.c.]}$ (d). Applied fields are $\mu_0 H = 1$, 3, 5, 7, and 9 T, temperature was in all cases $T = 0.99 T_c$ and $j = 50\ \mathrm{A\,cm^{-2}}$. The highlighted areas in (c) and (d) contain the nonscalable range (see text).

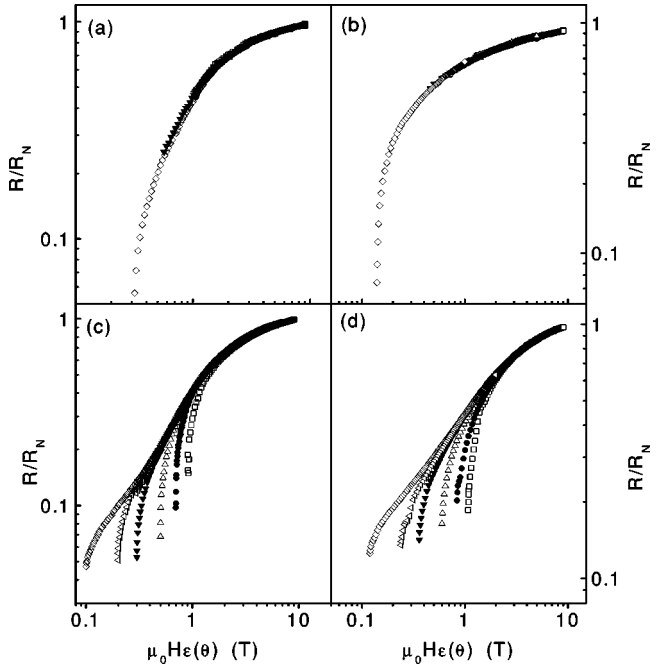

FIG. 2. Scaling of the angular dependent normalized resistance curves for applied fields $\mu_0 H = 1$, 2, 3, 5, 7, and 9 T, for samples YBCO 50 nm (a), $YBCO_{[17\ u.c.]}/PBCO_{[2\ u.c.]}$ (b), $YBCO_{[8\ u.c.]}/PBCO_{[5\ u.c.]}$ (c), and $YBCO_{[5\ u.c.]}/PBCO_{[5\ u.c.]}$ (d). Note the nonscalable points in (c) and (d).

applied in directions close to YBCO/PBCO interface (or Cu-O planes), being dissipation highly reduced in the case of the decoupled superlattices.

We have used the scaling approach for three-dimensional (3D) anisotropic superconductors proposed by Blatter *et al.*[15] to analyze the anisotropic behavior of the superlattices and the YBCO single film. This model gives a scaling rule that allows collapsing angular dependent resistance $R(\theta,H)$ curves into a single curve in terms of a reduced field $R(H_\varepsilon)$. H_ε is defined as $H_\varepsilon = H\varepsilon(\theta)$, where the scaling factor $\varepsilon(\theta) = H_{c_2}(\theta)/H_{c_2}^{a,b}$, in particular, we use

$$\varepsilon(\theta) = \sqrt{\sin^2(\theta) + \gamma^{-2}\cos^2(\theta)} \tag{1}$$

with the anisotropy parameter $\gamma = H_{c_2}^{a,b}/H_{c_2}^{c}$. It is important to remark that, within this model, no assumptions are made about the dissipation mechanisms, neither on its dependence on field, angle, or temperature.[7] Following this formalism, we tried to collapse $R(\theta,H)$ curves depicted in Fig. 1 onto a single master curve for each sample, in terms of the simple free parameter γ. Results are shown in Fig. 2. Plots are in a double logarithmic scale to highlight deviations from the master curve or not-collapsed points. Thus, in the case of the YBCO single film, we have obtained good scaling with $\gamma \sim 7$, well in the range $\gamma \sim 5-10$ reported in the literature.[16,17] The same behavior is observed for the coupled superlattice, which is well described within a 3D model with a similar anisotropy parameter $\gamma \sim 7$. However, in the case of the decoupled superlattices it is not possible to scale down dissipation over the whole angular range, i.e., no value of the anisotropy γ allows collapsing points from $R(\theta,H)$ curves in the range $20° < \theta < 20°$ [highlighted area in Figs. 1(c) and 1(d)]. Good scaling is achieved out of this angular range, consistent with an anisotropy parameter $\gamma \sim 7$. Dissipation in the range $20° < \theta < 20°$ is lower than expected from the anisotropic ($\gamma \sim 7$) 3D behavior occurring in the remaining range $20° < \theta < 170°$.

It is well known that resistivity is thermally activated in the TAFF regime (thermally activated flux flow),[1]

$$\rho = \rho_0 \exp\left(\frac{-U(H,T,\theta)}{K_B T}\right). \tag{2}$$

Therefore, to get further insight into this anomalous behavior, we have investigated the field dependence of the activation energies.

Following the 3D anisotropic model, the angular and field dependent activation energy $U(\theta,H,T)$ can be described by[18,19]

$$U(\theta,H,T) = U_0(\theta,H)\left(1 - \frac{T}{T_c}\right) = \frac{\beta}{(H\varepsilon(\theta))^\alpha}\left(1 - \frac{T}{T_c}\right). \tag{3}$$

Where β is an energy scale, α gives field dependence, and the anisotropy γ is included in $\varepsilon(\theta)$ [see Eq. (1)]. Since we got γ from the scaling of $R(\theta,H)$ curves, β and α can be obtained from fits of $\ln[R(\theta,H)]$ to Eq. (3). It is worth noting that, once γ is known, the shape of the curve $U(\theta,H)$ only depends on α. In this way, we have extracted $U_0(\theta,H)$ from the $R(\theta,H)$ curves shown on Fig. 1, and the results are de-

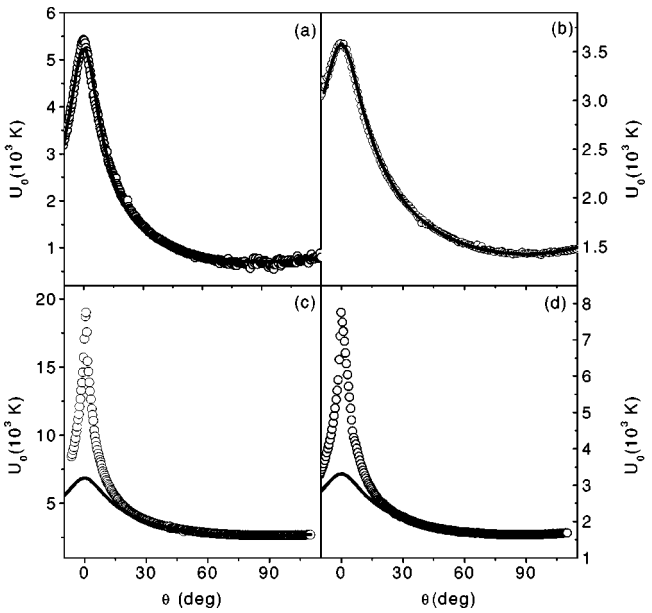

FIG. 3. Activation energies as a function of angle for samples $YBCO_{50\ nm}$ (a), $YBCO_{[17\ u.c.]}/PBCO_{[2\ u.c.]}$ (b), $YBCO_{[8\ u.c.]}/PBCO_{[5\ u.c.]}$ (c), and $YBCO_{[5\ u.c.]}/PBCO_{[5\ u.c.]}$ (d), in applied field $\mu_0 H=9$ T. Circles are experimental data, and solid lines are best fits to Eq. (3).

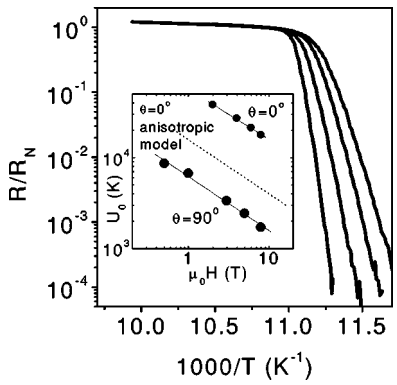

FIG. 4. Superconducting transitions of sample $YBCO_{[8\ u.c.]}/PBCO_{[5\ u.c.]}$ in applied field of $\mu_0 H=2$, 4, 6, and 8 T parallel to YBCO/PBCO interfaces. Inset: Activation energies as a function of applied field, for fields applied parallel to YBCO/PBCO interface (upper curve), and parallel to *c* axis (below).

picted in Fig. 3. In the case of the YBCO single films, nice fits are obtained yielding $\alpha\sim 1$, while for the coupled superlattice we have found $\alpha\sim 0.5$. In the case of the decoupled superlattices, we applied the above analysis only to the angular range where the 3D anisotropic model works, namely, $20°<\theta<170°$, and using the value $\gamma\sim 7$ obtained from the scaling analysis of Fig. 2, we got $\alpha\sim 0.5$. This is shown in Figs. 3(c) and 3(d), where one can see that the experimental values of the activation energy for $\theta=0$ are almost about three times higher than expected from the extrapolation of the fits to Eq. (3) at $\theta=0$ (solid line).

Since, for the decoupled superlattices, the dependence of the activation energy on field (given by α) cannot be inferred from the above procedure when field is applied in directions close to YBCO/PBCO interfaces ($-20°<\theta<20°$), we measured $R(T,H)$, in both field parallel to Cu-O planes ($\theta=0$) and field parallel to *c*-axis ($\theta=90$). Results for $\theta=0$ are shown in Fig. 4, in an Arrhenius plot. The activation energies $U_0(H)$ (depicted in the inset of Fig. 4) were obtained from the linear portions of the Arrhenius plots. U_0 displays an inverse square-root dependence $U_0\propto H^{-0.5}$ ($\alpha\sim 0.5$), for both $\theta=0$ and $\theta=90$, i.e., the activation energy dependence on H does not change with field orientation, excluding this as an origin of the dissipation anomaly at low angles.

In the case of YBCO single film and *c*-axis coupled superlattice, pinning effects arising from the layered structure dominate over the whole angular range, in a way that angular dependent dissipation can be scaled in terms of an effective field H_ε by means of the factor $\varepsilon(\theta)$. However, for *c*-axis decoupled superlattices, another pinning mechanism arises that overcomes the intrinsic one when field is applied in directions in the range $-20°<\theta<20°$ (close to YBCO/PBCO interfaces). This barrier for flux motion is only active in this angular range, giving rise to a reduced dissipation, while it does not affect vortex motion when field is applied in the range $20°<\theta<170°$, where dissipation becomes scalable with the 3D anisotropic model. The physical origin of these interface related barriers in *c*-axis superlattices is clearly connected with the fact that YBCO layers are fully decoupled by the 5 unit cells PBCO spacer. This point was well established by experiments on the dependence of the activation energy U_0 on PBCO spacer thickness;[12,14]; it was found that U_0 saturated with a spacer thickness of 4 PBCO unit cells or higher, showing that this PBCO thickness was enough to fully decouple YBCO layers. The same result was obtained from the T_c dependence on PBCO spacer thickness *n* in the *c*-axis superlattices series $YBCO/PBCO_{[n\ u.c.]}$,[13] since T_c was found independent of PBCO thickness above four unit cells. Another point, which should be addressed, is the role played by the PBCO layers. In the case of *a*-axis oriented superlattices (Cu-O planes perpendicular to the substrate) the effects of both, intrinsic pinning and PBCO layers pinning, could be easily separated. Velez *et al.* have shown that, contrary to our observation, vortex pinning at PBCO in *coupled a*-axis superlattices displays an angular dependent resistance scaling following a 3D model with a given anisotropy parameter γ.[20,21] In this case, vortex pinning even stronger than intrinsic pinning takes place in the PBCO spacer, where the order parameter is not completely suppressed, since the superconducting layers are coupled. In our case, however, we did not found any γ value that allowed scaling down dissipation in the whole angular range for the *c*-axis decoupled superlattices. Therefore, vortex trapping in PBCO layers has to be discarded as the origin of the anomalous reduced dissipation in parallel applied magnetic field in decoupled superlattices.

In view of the above considerations, we can think of the decoupled superlattices as a stack on thin independent superconducting slabs (YBCO layers) separated by nonsuperconducting (insulator) PBCO. When magnetic field is applied close to parallel to the YBCO/PBCO interface, the magnetic field would enter PBCO layers as magnetic field lines and YBCO layers as vortices. In such situation, reduced dissipa-

tion is most likely due to vortex trapping at the YBCO layers instead of at PBCO layers. The mechanism responsible for this may be related to the so-called Bean-Livingston (BL) or surface barriers,[9] whose importance in the magnetic and electric behavior of HTCS has been experimentally addressed during the last years.[22–28] The physical origin of these barriers lies on two contributions: on one hand, the vortex-antivortex (mirror image outside the sample) interaction, which results in attractive force to the surface (barrier for flux entry). On the other hand, there is the repulsive Lorentz force on the vortex caused by shielding supercurrents in presence of applied magnetic field (barrier for flux escape). When field is applied parallel to YBCO/PBCO interface, the YBCO/PBCO interface behaves as a *surface*. A similar scenario has been theoretically examined by Burlachkov *et al.*,[29] i.e., surface pinning in a HTCS superconducting slab in parallel magnetic field. In that paper, the effects of surface pinning at equilibrium magnetization on transport properties are addressed by taking into account the vortex-surface interaction in addition to the vortex-vortex interaction. This yields a characteristic length over which vortices should feel surface influence of the order of $a_0 \simeq (\phi_0/\gamma B)^{0.5}$ which, taking into account our experimental data range, is always larger than 6 nm (a_0 value for 9 T), and thus of the order or larger than YBCO layer thickness in the decoupled superlattices. Within a_0 surface effects should overcome intrinsic ones if BL barriers are higher than intrinsic ones. Always following the work of Burlachkov *et al.*[29] the dissipation in the equilibrium vortex liquid state dominated by surface effects is linear (Ohmic), yielding an Arrheniuslike resistance law, as in the TAFF [Eq. (2)], with an activation energy given by $U(H,T) = \phi_0 \lambda m_{eq}^{3/2}/4\pi\sqrt{\gamma^2 H}$, where m_{eq} is the equilibrium magnetization and ϕ_0 the flux quanta. Using typical values for YBCO, $\lambda = \lambda_0/\sqrt{1-(T/T_c)^4}$ and $\lambda_0 = 140$ nm (penetration depth), $\gamma \sim 7$ (anisotropy parameter) and $\mu_0 H \approx B$, Burlachkov *et al.*[29] give an estimate for $U_0 \approx 5\times 10^4/\sqrt{B}$ K (with B in T). Therefore, BL barriers contribution to transport properties is expected in the case of ultrathin YBCO layers in decoupled superlattices with individual layer thickness of the order of a_0, which points to this mechanism as the responsible for the reduced dissipation observed in these samples in applied magnetic fields parallel to YBCO/PBCO interfaces. Moreover activation energies are within the order of magnitude estimated by Burlachkov *et al.*[29] and exhibit the correct $(1/\sqrt{B})$ magnetic field dependence. Notice that the behavior of both decoupled samples $YBCO_{[5\ u.c.]}/PBCO_{[5\ u.c]}$ and $YBCO_{[8\ u.c.]}/PBCO_{[5\ u.c.]}$ is similar [Figs. 3(c) and 3(d)] despite the number of interfaces is almost twice in the $YBCO_{[5\ u.c.]}/PBCO_{[5\ u.c.]}$ superlattice. This can be understood considering that YBCO layers in the superlattice are fully decoupled, and thus the observed behavior is in fact the same that could be expected for a single YBCO layer of identical thickness and perfect surfaces. Unfortunately in practice YBCO single films five unit cells thick exhibit depressed T_c values (60 K) compared to superlattices (80 K), resulting from surface imperfections and exposure to ambient conditions,[30] and thus comparison of the dissipation properties is meaningless. BL barrier effects are not observed in the coupled superlattice since the relevant length scale to compare with a_0 is sample thickness (200 nm). On the other hand, $YBCO_{50\ nm}$ single films have rough surfaces resulting from a 3D growth mode for these large thickness. Surface imperfections (steps, grain boundaries, etc.) with sizes comparable to coherence length ξ wash out BL barriers.[9,29] Accordingly, the absence of BL mechanism contribution to the transport properties of the coupled superlattice and the $YBCO_{50\ nm}$ single film is expected.

In summary, decoupled *c*-axis YBCO/PBCO superlattices show strongly reduced dissipation in applied fields parallel to the YBCO/PBCO interfaces, while coupled superlattice behaves similar to single films, following an anisotropic 3D angular dependent dissipation. For decoupled superlattices, the fact that YBCO layers thickness are comparable with the characteristic length in which BL barriers affect vortices, together with the sharpness of YBCO/PBCO interface results in geometry which is suited to strengthen their effects. We point to this mechanism as the one governing dissipation in applied fields close to parallel to interfaces.

We acknowledge financial support from Spanish CICYT through Grants Nos. MAT2002-4543 and MAT2000-1468, Grant No. CAM 07N/0008/2001, ESF-Vortex Program, and R. Areces Foundation. One of us (E.M.G.) wants to thank Ministerio de Ciencia y Tecnología for a Ramon y Cajal contract.

*Present address: Condensed Matter Science Div. Oak Ridge National Laboratory.

[1] G. Blatter, M.V. Feigel'man, V.B. Geshkenbein, A.I. Larkin, and V.M. Vinokur, Rev. Mod. Phys. **66**, 1125 (1994).

[2] F. Bouquet, C. Marcenat, E. Steep, R. Calemczuk, W.K. Kwok, U. Welp, G.W. Crabtree, R.A. Fisher, N.E. Phillips, and A. Schilling, Nature (London) **411**, 448 (2001).

[3] M. Tachiki and S. Takahashi, Solid State Commun. **70**, 291 (1989).

[4] S.N. Gordeev, A.A. Zhukov, P.A.J. de Groot, A.G.M. Jansen, R. Gagnon, and L. Taillefer, Phys. Rev. Lett. **85**, 4594 (2000).

[5] For a review, see J.M. Triscone and Ø. Fischer, Rep. Prog. Phys. **60**, 1673 (1997).

[6] X.G. Qiu, G.X. Chen, B.R. Zhao, V.V. Moshchalkov, and Y. Bruynseraede, Phys. Rev. B **68**, 024519 (2003).

[7] E.M. Gonzalez, J.M. Gonzalez, and J.L. Vicent, Phys. Rev. B **62**, 8707 (2000).

[8] E.M. Gonzalez, J.E. Villegas, M. Varela, J. Santamaria, Ivan P. Prieto, K. Schuller, and J.L. Vicent, Appl. Phys. Lett. **80**, 3994 (2002).

[9] C.P. Bean and J.D. Livingston, Phys. Rev. Lett. **12**, 14 (1964).

[10] M. Varela, Z. Sefrioui, D. Arias, M.A. Navacerrada, M. Lucía, M.A. López de la Torre, C. León, G.D. Loos, F. Sánchez-Quesada, and J. Santamaría, Phys. Rev. Lett. **83**, 3936 (1999).

[11] M. Varela, W. Grogger, D. Arias, Z. Sefrioui, C. León, C. Ballesteros, K.M. Krishnan, and J. Santamaría, Phys. Rev. Lett. **86**, 5156 (2001).

[12] O. Brunner, L. Antognazza, J.-M. Triscone, L. Miéville, and Ø. Fischer, Phys. Rev. Lett. **67**, 1354 (1991).

[13] M. Varela, D. Arias, Z. Sefrioui, C. León, C. Ballesteros, and J.

Santamaría, Phys. Rev. B **62**, 12 509 (2000).
[14] H.C. Yang, L.M. Wang, and H.E. Horng, Phys. Rev. B **59**, 8956 (1999).
[15] G. Blatter, V.B. Geshkenbein, and A.I. Larkin, Phys. Rev. Lett. **68**, 875 (1992).
[16] D.E. Farrell, J.P. Rice, D.M. Ginsberg, and J.Z. Liu, Phys. Rev. Lett. **64**, 1573 (1990).
[17] Z. Sefrioui, D. Arias, E.M. Gonzalez, C. Leon, J. Santamaría, and J.L. Vicent, Phys. Rev. B **63**, 064503 (2001).
[18] X. Xiaojun, F. Lan, W. Liangbin, Z. Yuheng, F. Jun, C. Xiaowen, L. Kevin, and S. Hisashi, Phys. Rev. B **59**, 608 (1999).
[19] T. Puig and X. Obradors, Phys. Rev. Lett. **84**, 1571 (2000).
[20] J.I. Martín, M. Velez, and J.L. Vicent, Phys. Rev. B **52**, R3872 (1995).
[21] M. Vélez, E.M. González, J.I. Martín, and J.L. Vicent, Phys. Rev. B **54**, 101 (1996).
[22] M. Konczykowski, L.I. Burlachkov, Y. Yeshurun, and F. Holtzberg, Phys. Rev. B **43**, 13 707 (1991).
[23] L. Burlachkov, Y. Yeshurun, M. Konczykowski, and F. Holtzberg, Phys. Rev. B **45**, 8193 (1992).
[24] F. Zuo, D. Vacaru, H.M. Duan, and A.M. Hermann, Phys. Rev. B **47**, 5535 (1993).
[25] J.A. Lewis, V.M. Vinokur, J. Wagner, and D. Hinks, Phys. Rev. B **52**, R3852 (1995).
[26] D.T. Fuchs, E. Zeldov, M. Rappaport, T. Tamegai, S. Ooi, and H. Shtrikman, Nature (London) **391**, 373 (1998).
[27] A. Mazilu, H. Safar, D. López, W.K. Kwok, G.W. Crabtree, P. Guptasarma, and D.G. Hinks, Phys. Rev. B **58**, R8913 (1998).
[28] D.T. Fuchs, R.A. Doyle, E. Zeldov, S.F.W.R. Rycroft, T. Tamegai, S. Ooi, M.L. Rappaport, and Y. Myasoedov, Phys. Rev. Lett. **81**, 3944 (1998).
[29] L. Burlachkov, A.E. Koshelev, and V.M. Vinokur, Phys. Rev. B **54**, 6750 (1996).
[30] M. Varela, W. Grogger, D. Arias, Z. Sefrioui, C. León, L. Vazquez, C. Ballesteros, K.M. Krishnan, and J. Santamaria, Phys. Rev. B **66**, 174514 (2002).